Innovative Approach to Meet NYC System Reliability and Resilience Needs

Ed Wah Chen, Anastasia O'Malley, Nadia Ali,
Leslie Philp, Diego Pichardo, and Fabricio Mantilla
Consolidated Edison Company of New York, Inc.

Rogerio Scharlach and Satish Samineni
Schweitzer Engineering Laboratories, Inc.

Presented at the
45th Annual Western Protective Relay Conference
Spokane, Washington
October 16–18, 2018

Innovative Approach to Meet NYC System Reliability and Resilience Needs

Ed Wah Chen, Anastasia O'Malley, Nadia Ali, Leslie Philp,
Diego Pichardo, and Fabricio Mantilla, *Consolidated Edison Company of New York, Inc.*
Rogerio Scharlach and Satish Samineni, *Schweitzer Engineering Laboratories, Inc.*

***Abstract*—Consolidated Edison Company of New York, Inc. (Con Edison) services over 9 million customers in New York City and has long been recognized throughout the utility industry for its reliable and robust electrical system. Con Edison relentlessly focuses on improving its system and, more importantly, mitigating risks and overcoming unexpected equipment losses that may occur. Recent weather events, equipment failures, and past terrorist events are among the possible causes of unexpected equipment losses. With that in mind, Con Edison took the initiative to start their "Resiliency Transformer Project" in the summer of 2016. A staged public demonstration at the completion of the project took place in January 2017. Con Edison has been the first utility company in the United States to successfully energize and utilize these units.**

This paper discusses the concept of the "resiliency transformer," and its electrical and physical characteristics, as well as functional features that improve system flexibility during emergencies. It explains how the use of state-of-the-art digital secondary systems that are simple, flexible, and secure helped in rapid deployment of transformer protection. It also discusses aspects related to the design of mobile relay panels, the demonstration and staging of the units, digital simulations, and commissioning.

I. Introduction

Consolidated Edison Company of New York, Inc. (Con Edison) is one of the largest investor-owned utilities in the world. Founded in 1823 as the New York Gas Light Company, Con Edison provides electric, gas, and steam services to 9 million customers over 604 square miles of New York City (NYC) and Westchester County in New York [1]. Con Edison owns approximately 94,000 miles of underground cable and 34,000 miles of overhead conductors. In 2017, NYC consumed 52,266 GWh of electricity, which constituted 33 percent of New York's total electricity consumption [2].

Because of its highly dense service territory, Con Edison operates one of the most complex and unparalleled electric systems in the world while still providing the most reliable electric services to customers in NYC.

System disturbances and interruptions (such as equipment failure, terrorism, vandalism, storms, and/or floods) can occur at any time. When disasters do occur, it can be a challenge to expedite restoration because of long lead times for replacement equipment. For example, large transmission-level power transformers can have a lead time of 12 to 18 months. Additionally, it can take several weeks to transport a large transformer to a substation and install it onsite. A project team was formed with a group of engineers from various technical departments to find a solution to this problem.

This project team started the "Resiliency Transformer Project." They designed a power transformer that is lightweight for transportation, compact for confined spaces in the substation, and flexible for a simple and fast connection to the existing power system. The power transformer also has various transmission voltage tap selections. The team used a new digital secondary system as part of the protection system. This system provides protection engineers and field technicians with simplicity and flexibility, lowers costs, and reduces cybersecurity threats.

II. Resiliency Transformer

Engineers at Con Edison partnered with their power transformer equipment manufacturers to develop an innovative, transmission-level mobile resiliency transformer for quick installation to help ensure grid resiliency.

Rather than completely replacing a power transformer in a two-week time frame, we designed a transformer that can allow a replacement to be made in three days or less. Three single-phase transformers and their associated accessories can be delivered to a substation, and then, a few days later, the replacement transformer can be plugged in and energized.

The resiliency transformer design features enable flexible operation and quick installation. The transformer was designed as three single-phase transformers to minimize the shipping weight and dimensions, making transportation easier. In addition, it was designed with a hybrid insulation system that uses high-temperature materials such as aramid, conductor insulation and synthetic ester, and dielectric fluid. This high-temperature insulation system reduces the winding dimensions and cooling requirements. Rather than using traditional radiators, the transformer uses forced oil-to-air coolers, which have a smaller footprint. These coolers are already mounted and fully interconnected to the transformer main tank. Synthetic ester has a higher fire point than mineral oil, so it reduces fire risks. In addition, synthetic ester is readily biodegradable, while mineral oil has very little biodegradability.

Because of the environmentally friendly, biodegradable dielectric fluid, the transformer can be transported while filled. The transformer is equipped with two-part, plug-in bushings and cable connections. The plug-in bushings expedite installation by eliminating the need to drain the dielectric fluid

before installing the bushing connections and then subsequently drying and refilling the transformer. The transformer primary connection to the substation overhead bus is made with the two-part, plug-in bushing. The transformer secondary connection can be made either with a two-part, plug-in bushing connection to the overhead bus or with a plug-in cable connection with a portable pothead stand. This feature offers flexibility in positioning the transformer within the substation to interconnect with the electric system.

The control cable connections between the individual phase units and the common control cabinet are made with cables that have color-coded military specification plug-in cable connectors. The common control cabinet with the cable reels, power cables, portable pothead stands, and bushings are containerized for easy transport and quick, modular installation.

The transformer was designed for flexible operation and can be used to replace a majority of installed transmission transformers. It has dual ratings and can be operated at either 300 MVA for a 335/136 kV transformer or at 150 MVA for a 134/69 kV transformer. A de-energized tap changer allows for operating mode selection, and the tap can be changed without having to handle dielectric fluid and enter the transformer to change internal electrical connections. In addition, the transformer is designed to have a high-overload capability (up to 170 percent of the nameplate rating during the summer). It is also designed as a low-noise unit (78 dBA) to minimize disturbances.

To prove how the new transformer concept works, a demonstration was performed where an existing 328 MVA, 345/138 kV autotransformer was replaced with the mobile resiliency transformer (see Fig. 1). The resiliency transformer was placed on the surveyed lines at the proper location, and the plug-in bushings and secondary cable connections were made. The portable pothead stands were used for interconnection with the secondary 138 kV bus. The common control cabinet was installed, and the interconnecting control cables were set up. The final verification tests and safety checks were performed, and the transformer was energized in less than three working days, verifying the resiliency concept.

Fig. 1. Mobile Resiliency Transformers Deployed to Replace a 328 MVA, 345/138 kV Autotransformer

III. Digital Secondary System

A transmission or distribution substation is composed of power equipment, such as disconnect switches, circuit breakers, power transformers, buses, line traps, surge arresters, instrument transformers, and so on. The active parts of these devices (such as circuit breaker contacts, power transformer windings, and potential transformer primary windings) are in contact with high voltages and are part of the primary system. The secondary system is also present in substations. It is isolated from the primary system and operates at low-voltage levels. The secondary windings of instrument transformers are part of the secondary system. The analog information that the instrument transformers generate has been traditionally transmitted to the substation control house via copper wires. Protective relays, remote terminal units (RTUs), and protection and control systems use this information.

In a digital secondary system, the analog information generated by the secondary windings of the instrument transformers is digitized at the point of collection by a merging unit (MU) and transmitted to the substation control house via fiber-optic cables. Purpose-built protective relays, RTUs, and protection and control systems use the digitized information to protect, control, and automate the substation.

Two basic architectures for the digital secondary system were considered for the resiliency transformer project: switched network and point-to-point. Switched network architectures require MUs located near the primary equipment to sample the analog signals and publish the data to the network. This architecture also requires network switches, a time-synchronizing clock, and intelligent electronic devices (IEDs) to consume the data. Point-to-point architectures require MUs and IEDs to consume the data.

Switched network architectures require more equipment connections than point-to-point architectures. Switched network architectures require connections between the MUs and switches, the switches and IEDs, and the switches and the clock. Point-to-point architectures require a single direct-fiber connection between the MUs and IEDs. With fewer connections, point-to-point architectures are more reliable.

Point-to-point architectures eliminate the need for switches and complex network engineering. With the possibility of preconfigured analog mapping topologies, point-to-point architectures provide easy mapping of the analog inputs from the MUs to the internal relay logic, reducing the cost and the complexity of system configuration.

Because analog-to-digital (A/D) conversion is performed at the MU, time synchronization is vital. The sampled analog signals must be time-aligned before they are used in some forms of protection (e.g., differential protection). In this case, accurate relative time is important for data alignment. In switched network architectures, relative time synchronization can be achieved with an IRIG-B or Precision Time Protocol (PTP) reference signal that is terrestrially distributed using a high-quality synchronous optical network or derived from sources, such a Global Positioning System (GPS) or Global Navigation Satellite System (GLONASS). Point-to-point architectures with fixed latencies and well-controlled jitters do not require external time sources to maintain relative time synchronization.

Switched network architectures use IEDs, MUs, clocks, and switches. Due to the large number of devices involved, there

are more points of access to the network, increasing the risk of cyber attacks. Because point-to-point architectures do not have switches or clocks, and a direct link exists between the MUs and IEDs, they are inherently cybersecure.

An EtherCAT-based digital secondary system with point-to-point architecture was selected to meet the project needs for a simple, flexible, cost-effective, and cybersecure protection system for the resiliency transformer. The EtherCAT protocol is described in IEC 61158. Its focus on short cycle times, low jitter, and synchronization accuracy align with the requirements to implement a digital secondary system.

The selected microprocessor-based transformer differential relay is equipped with eight 100BASE-FX fiber EtherCAT ports that can be connected on a point-to-point configuration to a maximum of eight MUs. Each MU performs A/D conversion of the signals generated by the secondary system. The transformer protective relay is equipped with traditional digital I/O boards for local use, with the remaining I/O allocated to the MUs. The relay offers a set of preconfigured topologies. The selected topology for this project allows for remote data acquisition of nine current channels, three voltage channels, and twelve digital inputs and control of eight digital outputs (see Fig. 2).

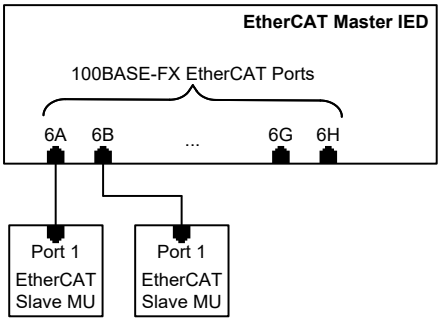

Fig. 2. Transformer Protective Relay and MU Topology

Once all the MUs are connected to the relay, the startup process is initiated by pressing the commissioning button near EtherCAT Port 6A. This process verifies that the connected ports and MUs are installed according to one of the supported topologies. Simultaneously, a single, predefined packet is created and is passed through the relay and the MUs. Once the startup process is completed, the topology is stored in memory. At each additional relay startup, the firmware validates that the connected modules match those of the stored configuration.

During operation, the EtherCAT packet is updated on the fly as it passes through the MUs and the relay. All the data is collected and aligned in the relay and made available to the protection, automation, and control functions. The relay sends synchronizing messages to all MUs using an internal clock as a reference. This allows each MU to synchronize its internal clock to the relay reference and synchronously sample the power system.

The test setup shown in Fig. 3 was used to evaluate the operating times of a conventional digital relay (Relay 1) and the digital relay with MUs (Relay 2). Both relays sample the power system at 8 kHz and process the protection elements 8 times per power system cycle, and they receive an IRIG-B signal for absolute time synchronization. A variable ac current source was used to inject current into the IAT channel of Relay 1 and the IAS and IAW channels of Relay 2. The current channels were connected in series. Instantaneous phase overcurrent elements were set to 10 A on all three current channels. Both relays were set to trigger event reports when the overcurrent elements asserted. The length of the event report was set at 30 cycles, and the pretrigger time was set to 6 cycles. The sampling rate for the COMTRADE event reports was set at 8 kHz. A 4 A pre-fault current was applied for 5 seconds, and 20 A fault current was applied for 10 cycles.

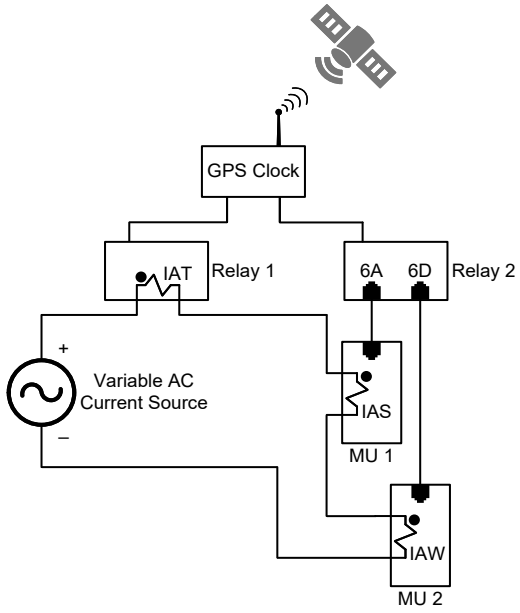

Fig. 3. Test Setup Demonstrates MU Relative Time Synchronization

Fig. 4 shows a plot generated with data from the COMTRADE event report that Relay 2 captured. Channels IAS and IAW are displayed on the same axis. Note that the sampled points, as expected, coincide. This proves that the relative time synchronization between the MUs is accurate.

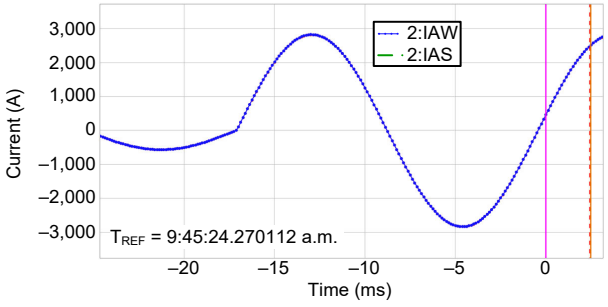

Fig. 4. Relative Time Synchronization

Fig. 5 shows a plot generated with data from the COMTRADE event reports that Relays 1 and 2 captured. Traces labeled 50TP1, 50SP1, and 50WP1 are the outputs of the instantaneous overcurrent elements for Channels T, S, and W, respectively. The difference in operating time of the elements for Channels T and S was 1.403 ms. The difference in element operating time for Channels T and W was 1.403 ms. Per relay specifications, the expected operating time for

elements 50S and 50W is delayed by a maximum of 1.5 ms due to channel delay.

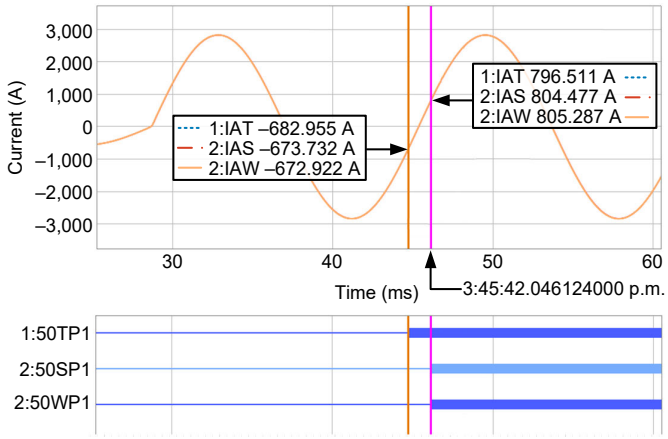

Fig. 5. Operating Time Differences

IV. Real-Time Digital Simulator (RTDS) Power System Model Setup

Fig. 6 shows the one-line diagram equivalent to the Con Edison power system that was modeled in an RTDS. The model consists of three single-phase, three-winding autotransformers rated at 335/136/13.8 kV. The tertiary winding is connected in delta and is unloaded. The autotransformer model parameters were derived from the transformer test reports. The autotransformers were modeled for core saturation.

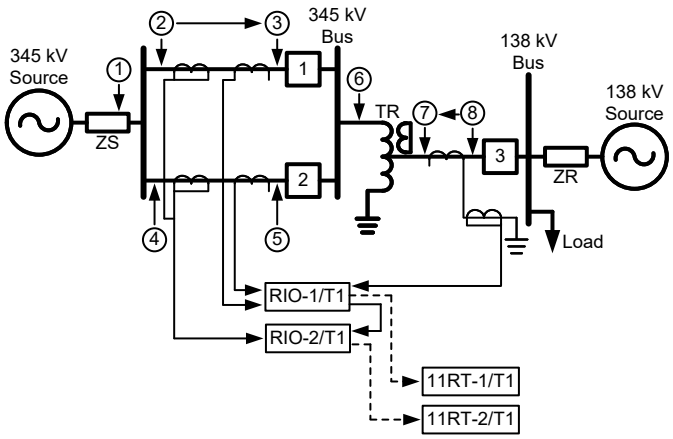

Fig. 6. RTDS Power System Model

High-voltage Breakers 1 and 2 and low-voltage Breaker 3 were interrupted during an autotransformer fault. Breaker 1 is modeled for point-on-wave open or close to control the magnitude of inrush currents. The current transformers (CTs) shown in Fig. 6 form the transformer differential protection zone. The CTs are modeled for simulating CT saturation by using data from the CT test reports.

Fig. 7 shows the laboratory setup. The low-level CT currents from the RTDS are amplified to true secondary currents using current amplifiers. These secondary currents are then fed to digital secondary protection system (DSPS) 1 (RIO-1/T1 and 11RT-1/T1) and DSPS 2, which provide transformer differential protection for the three autotransformers. The output contacts of DSPS 1 and 2 are wired to interface with the RTDS, thereby controlling Breakers 1, 2, and 3.

Eight fault locations were chosen for validating the protection system. Fault Locations 1, 2, 4, and 8 are external to the protection zone. Fault Locations 3, 5, 6, and 7 are internal. The model was configured to introduce 10 faults to any of these eight locations at various fault inception angles and fault resistances.

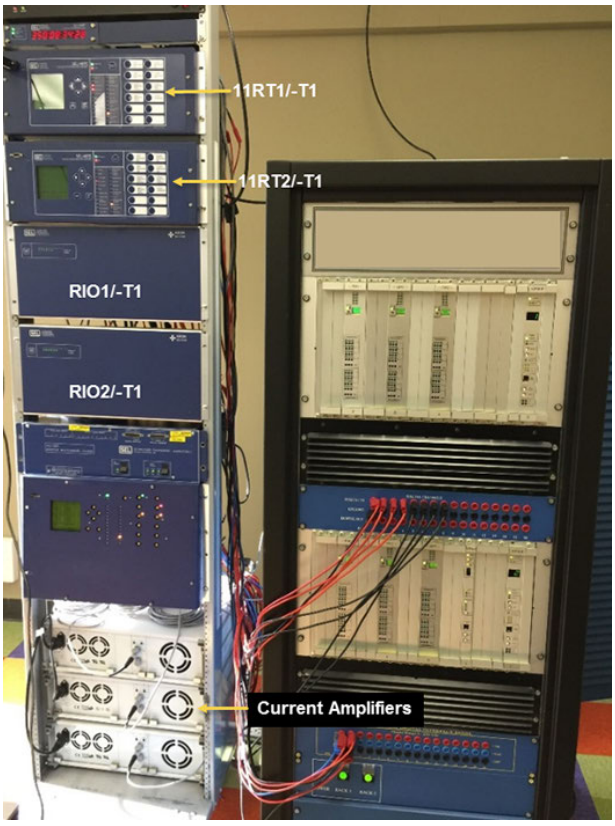

Fig. 7. RTDS Laboratory Setup

V. RTDS Validation Test Plan and Results

The DSPS protection performance was validated using Test Cases 1–15. This section shows the RTDS test results for these test cases. For each test case, there are two RTDS captures (one from DSPS 1 and the other from DSPS 2).

For Case 1, Breaker 1 is closed at the zero-degree point-on-wave bus voltage to cause maximum inrush on Phase A.

Fig. 8 shows the RTDS capture of DSPS 1 for Case 1. The first two analog graphs show the high-voltage-side CT secondary currents that are fed to Terminals S and T of DSPS 1. The third analog graph shows the low-voltage-side CT secondary currents that are fed to Terminal U of DSPS 2. Digital graphs with labels CB1, CB2, and CB3 indicate the respective breaker status. The digital graph labeled TRPXFMR_T1 indicates the DSPS 1 output contact (OUT101) state. The digital graphs labeled FLT1 through FLT8 indicate the location of the fault. The capture shows that when Breaker 1 is closed (CB1 is asserted), there is maximum inrush current on Phase A, and DSPS 1 was stable and did not trip (TRPXFMR_T1 stayed deasserted).

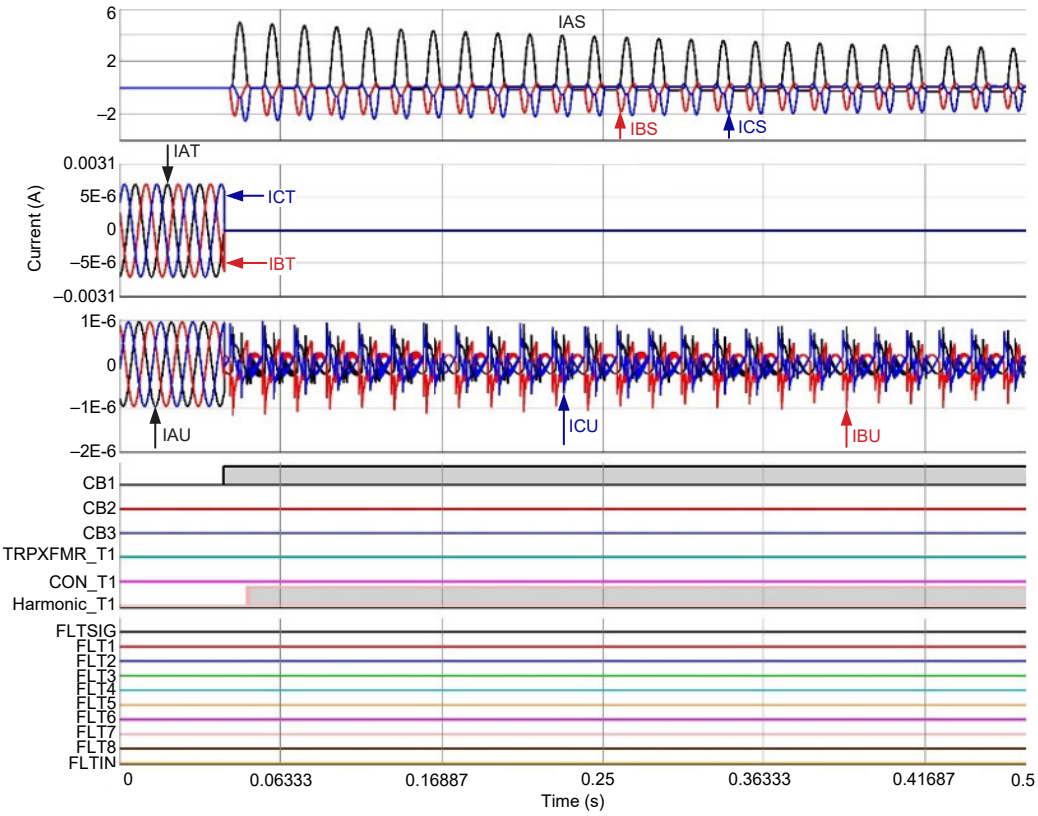

Fig. 8. Case 1: DSPS 1 Inrush Transients

Fig. 9 shows the RTDS capture of DSPS 2 for the same event shown in Fig. 8. The first analog graphs show the high-voltage-side CT secondary currents that are fed to Terminal S of DSPS 2. The second analog graph shows the low-voltage-side CT secondary currents that are fed to Terminal U of DSPS 2. The digital graph labeled TRPXFMR_T2 indicates the DSPS 2 output contact (OUT101) state. The digital graphs labeled FLT1 through FLT8 indicate the location of the fault. The capture shows that when Breaker 1 was closed (CB1 asserted), DSPS 2 was stable and did not trip (TRPXFMR_T2 stayed deasserted).

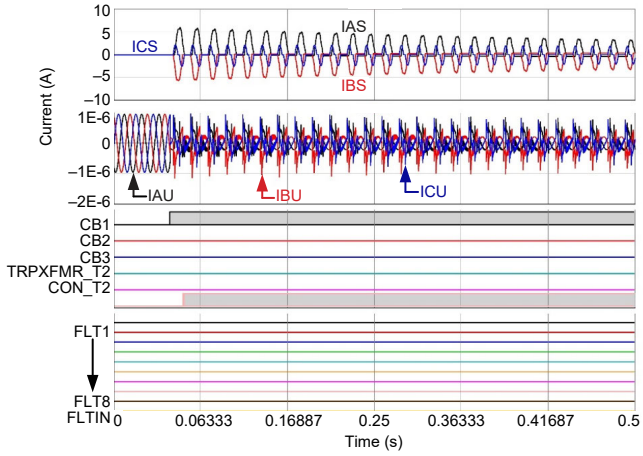

Fig. 9. Case 1: DSPS 2 Inrush Transients

For Case 2, we simulated an external Phase-A-to-ground (AG) fault at Location 1.

Fig. 10 shows the RTDS capture of DSPS 1 for Case 2. An external AG fault at Location 1 was initiated at 0.05 seconds and continues for 0.1 seconds. FLT1 asserted, indicating that the fault was at Location 1. The digital graph labeled CON_T1 indicates the DSPS 1 output contact (OUT102) state, which is mapped to the CON bit (external fault detection). The capture shows that CON_T1 asserted during the fault, indicating that it was an external fault. DSPS 1 switches to a secure slope for external faults. The capture shows that DSPS 1 stayed stable during the external AG fault and did not trip (TRPXFMR_T1 stayed deasserted).

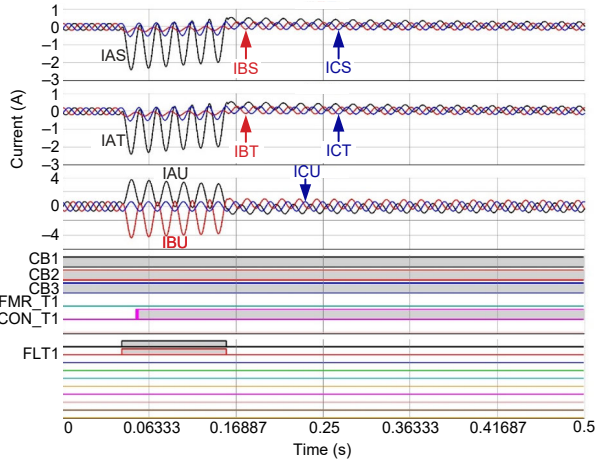

Fig. 10. Case 2: DSPS 1 External AG Fault at Location 1

Fig. 11 shows the RTDS capture of DSPS 2 for the same event shown in Fig. 10. FLT1 asserted, indicating that the fault was at Location 1. The digital graph labeled CON_T2 indicates the DSPS 2 output contact (OUT102) state, which is mapped to the CON bit (external fault detection). Fig. 11 shows that CON_T2 asserted during the fault, indicating that it was an external fault. DSPS 2 switches to a secure slope for external faults. The capture shows that DSPS 2 stayed stable during the external AG fault and did not trip (TRPXFMR_T2 stayed deasserted).

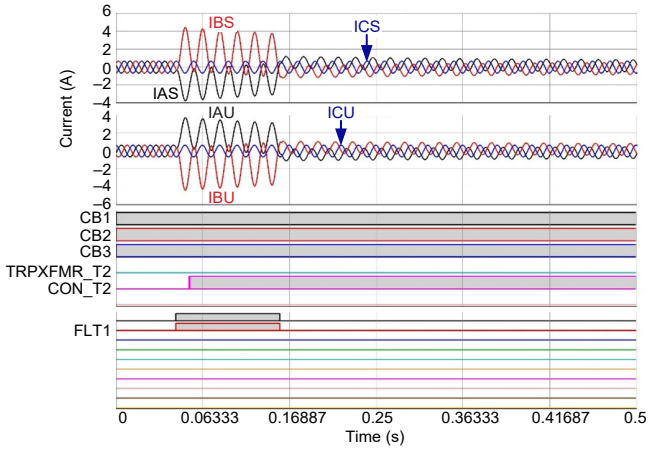

Fig. 11. Case 2: DSPS 2 External AG Fault at Location 1

For Case 3, we simulated an external AG fault at Location 2.

Fig. 12 shows the RTDS capture of DSPS 1 for Case 3. An external AG fault at Location 2 was initiated at 0.05 seconds and continued for 0.1 seconds. FLT2 asserted, indicating that the fault was at Location 2. Fig. 12 shows that CON_T1 asserted during the fault, indicating that it was an external fault. The capture shows that DSPS 1 stayed stable during the external AG fault and did not trip (TRPXFMR_T1 stayed deasserted).

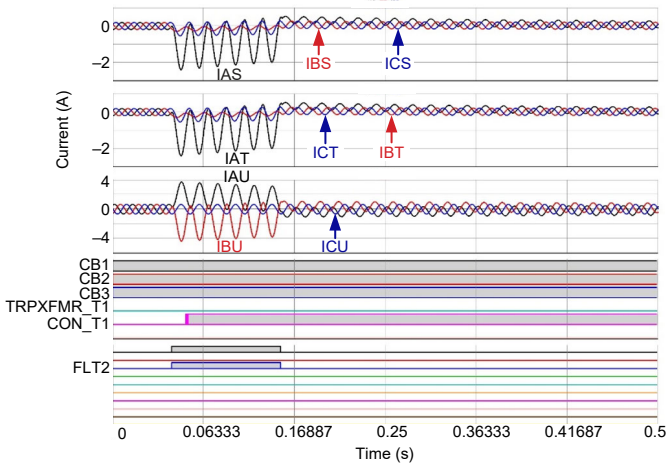

Fig. 12. Case 3: DSPS 1 External AG Fault at Location 2

Fig. 13 shows the RTDS capture of DSPS 2 for the same event shown in Fig. 12. FLT2 asserted, indicating that the fault was at Location 2. Fig. 13 shows that CON_T2 asserted during the fault, indicating that it was an external fault. The capture shows that DSPS 2 stayed stable during the external AG fault and did not trip (TRPXFMR_T2 stayed deasserted).

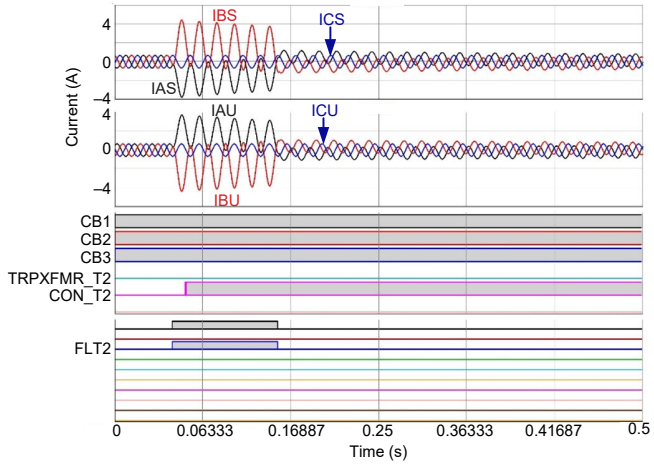

Fig. 13. Case 3: DSPS 2 External AG Fault at Location 2

For Case 4, we simulated an external AG fault at Location 4.

Fig. 14 shows the RTDS capture of DSPS 1 for Case 4. An external AG fault at Location 4 was initiated at 0.05 seconds and continued for 0.1 seconds. FLT4 asserted, indicating that the fault was at Location 4. Fig. 14 shows that CON_T1 asserted during the fault, indicating that it was an external fault. The capture shows that DSPS 1 stayed stable during the external AG fault and did not trip (TRPXFMR_T1 stayed deasserted).

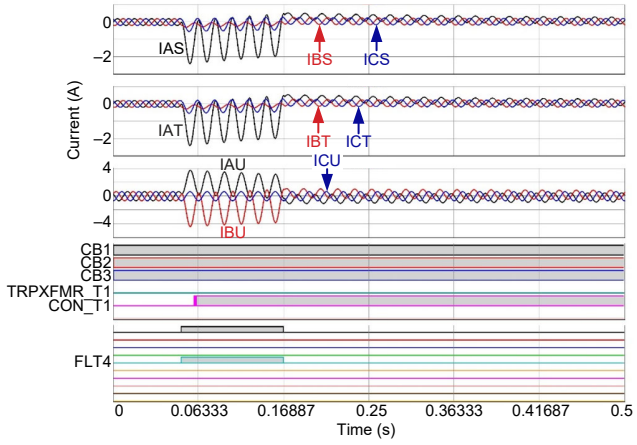

Fig. 14. Case 4: DSPS 1 External AG Fault at Location 4

Fig. 15 shows the RTDS capture of DSPS 2 for the same event shown in Fig. 14. FLT4 asserted, indicating that the fault was at Location 4. Fig. 15 shows that CON_T2 asserted during the fault, indicating that it was an external fault. The capture shows that DSPS 2 stayed stable during the external AG fault and did not trip (TRPXFMR_T2 stayed deasserted).

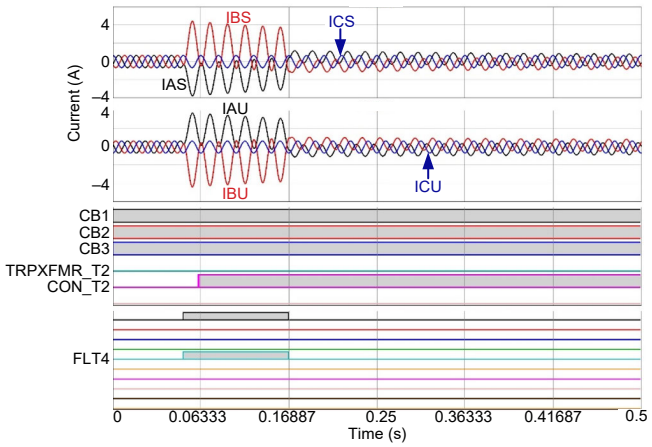

Fig. 15. Case 4: DSPS 2 External AG Fault at Location 4

For Case 5, we simulated an external AG fault at Location 8.

Fig. 16 shows the RTDS capture of DSPS 1 for Case 5. An external AG fault at Location 8 was initiated at 0.05 seconds and continued for 0.1 seconds. FLT8 asserted, indicating that the fault was at Location 8. Fig. 16 shows that CON_T1 asserted during the fault, indicating that it was an external fault. The capture shows that DSPS 1 stayed stable during the external AG fault and did not trip (TRPXFMR_T1 stayed deasserted).

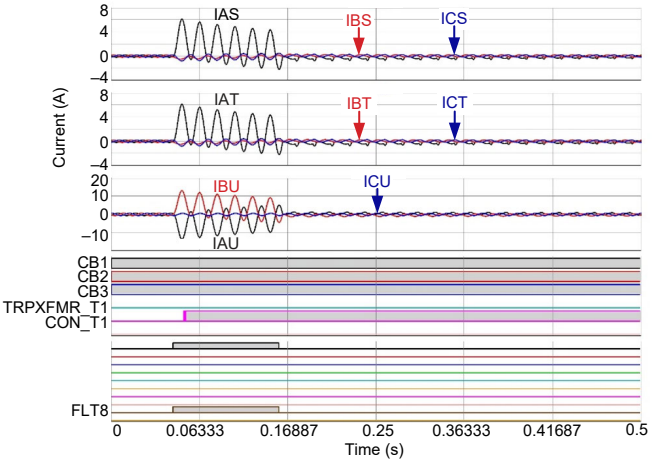

Fig. 16. Case 5: DSPS 1 External AG Fault at Location 8

Fig. 17 shows the RTDS capture of DSPS 2 for the same event shown in Fig. 16. FLT8 asserted, indicating that the fault was at Location 8. Fig. 17 shows that CON_T2 asserted during the fault, indicating that it was an external fault. The capture shows that DSPS 2 stayed stable for the external AG fault and did not trip (TRPXFMR_T2 stayed deasserted).

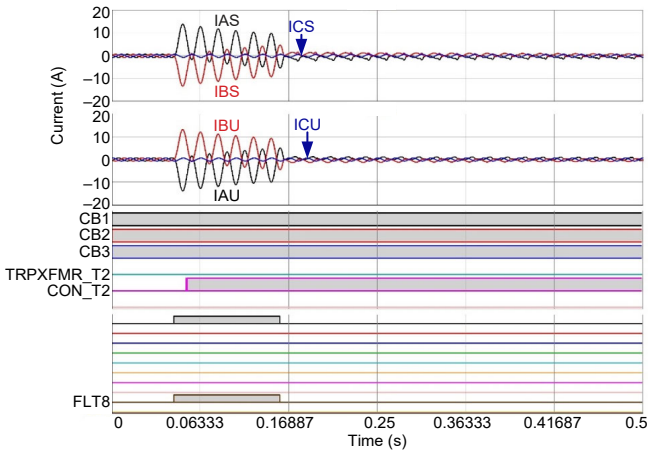

Fig. 17. Case 5: DSPS 2 External AG Fault at Location 8

For Case 6, we simulated an internal AG fault at Location 3.

Fig. 18 shows the RTDS capture of DSPS 1 for Case 6. An internal AG fault at Location 3 was initiated at 0.05 seconds and continued for 0.1 seconds. FLT3 asserted, indicating that the fault was at Location 3. Fig. 18 shows that DSPS 1 detected the internal fault (TRPXFMR_T1 asserted). DSPS 1 closed the output contact and tripped Breakers 1, 2, and 3.

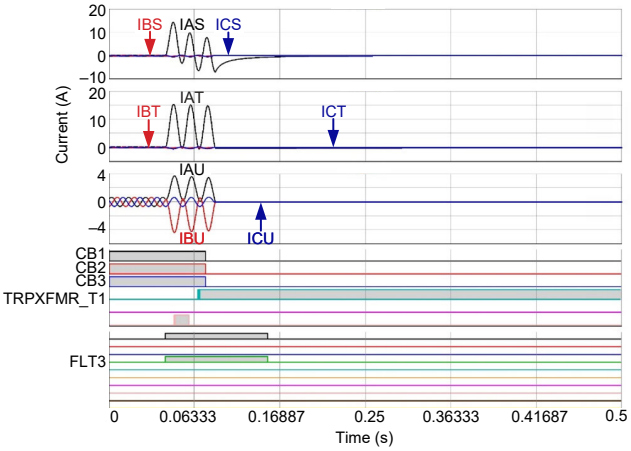

Fig. 18. Case 6: DSPS 1 Internal AG Fault at Location 3

Fig. 19 shows the RTDS capture of DSPS 2 for the same event shown in Fig. 18. Fig. 19 shows that DSPS 2 detected the internal fault (TRPXFMR_T2 asserted). DSPS 2 closed the output contact and tripped Breakers 1, 2, and 3.

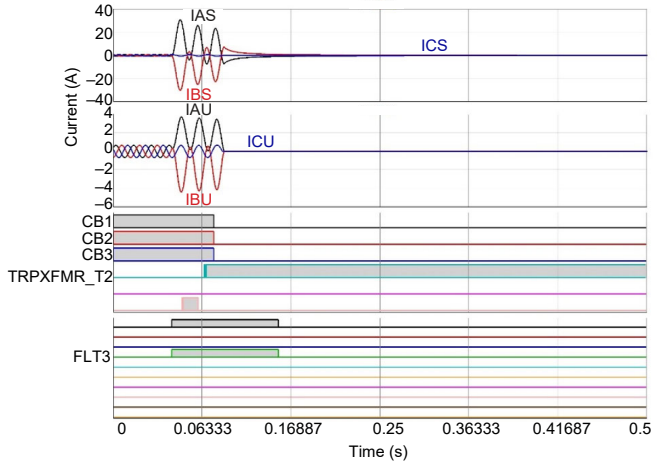

Fig. 19. Case 6: DSPS 2 Internal AG Fault at Location 3

For Case 7, we simulated an internal AG fault at Location 5. Fig. 20 shows the RTDS capture of DSPS 1 for Case 7. An internal AG fault at Location 5 was initiated at 0.05 seconds and continued for 0.1 seconds. FLT5 asserted, indicating that the fault was at Location 3. Fig. 20 shows that DSPS 1 detected the internal fault (TRPXFMR_T1 asserted). DSPS 1 closed the output contact and tripped Breakers 1, 2, and 3.

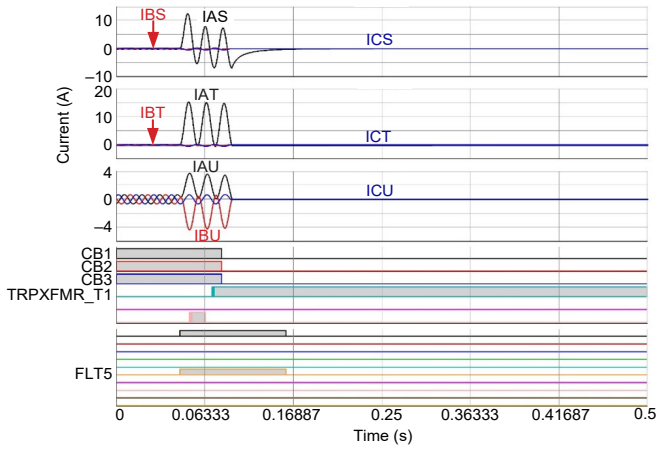

Fig. 20. Case 7: DSPS 1 Internal AG Fault at Location 5

Fig. 21 shows the RTDS capture of DSPS 2 for the same event shown in Fig. 20. Fig. 21 shows that DSPS 2 detected the internal fault (TRPXFMR_T2 asserted). DSPS 2 closed the output contact and tripped Breakers 1, 2, and 3.

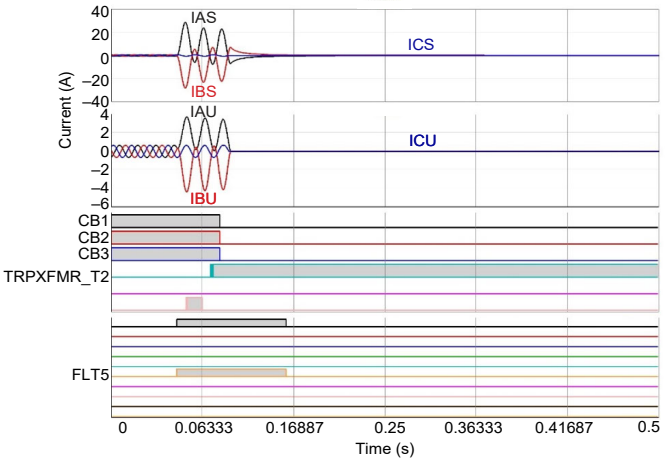

Fig. 21. Case 7: DSPS 2 Internal AG Fault at Location 5

For Case 8, we simulated an internal AG fault at Location 6. Fig. 22 shows the RTDS capture of DSPS 1 for Case 8. An internal AG fault at Location 6 was initiated at 0.05 seconds and continued for 0.1 seconds. FLT6 asserted, indicating that the fault was at Location 6. Fig. 22 shows that DSPS 1 detected the internal fault (TRPXFMR_T1 asserted). DSPS 1 closed the output contact and tripped Breakers 1, 2, and 3.

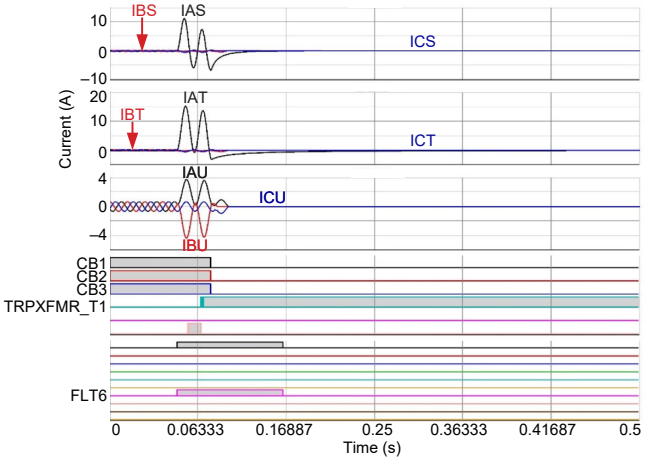

Fig. 22. Case 8: DSPS 1 Internal AG Fault at Location 6

Fig. 23 shows the RTDS capture of DSPS 2 for the same event shown in Fig. 22. Fig. 23 shows that DSPS 2 detected the internal fault (TRPXFMR_T2 asserted). DSPS 2 closed the output contact and tripped Breakers 1, 2, and 3.

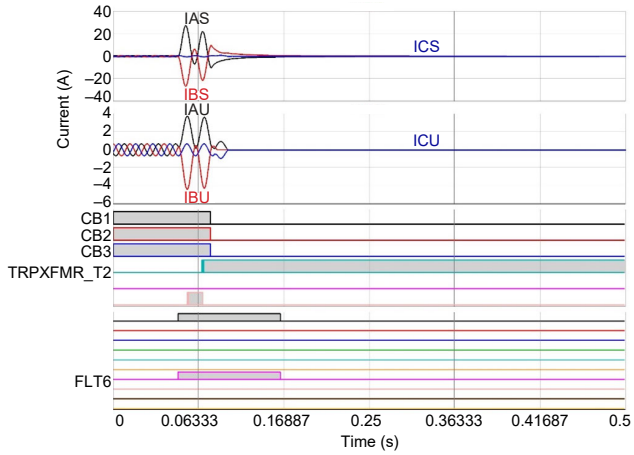

Fig. 23. Case 8: DSPS 2 Internal AG Fault at Location 6

For Case 9, we simulated an internal AG fault at Location 7.

Fig. 24 shows the RTDS capture of DSPS 1 for Case 9. An internal AG fault at Location 7 was initiated at 0.05 seconds and continued for 0.1 seconds. FLT7 asserted, indicating that the fault was at Location 7. Fig. 24 shows that DSPS 1 detected the internal fault (TRPXFMR_T1 asserted). DSPS 1 closed the output contact and tripped Breakers 1, 2, and 3.

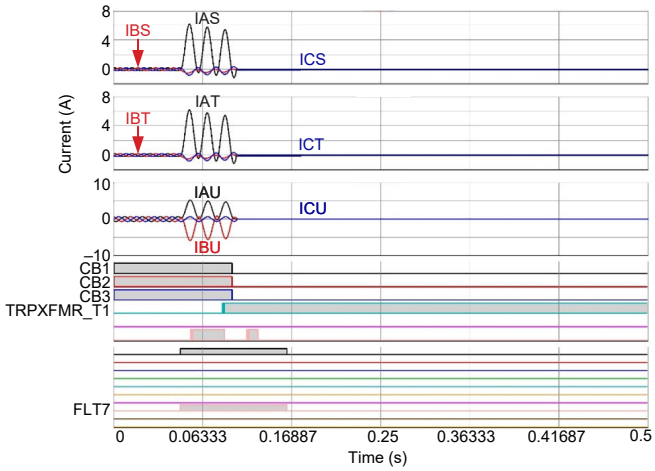

Fig. 24. Case 9: DSPS 1 Internal AG Fault at Location 7

Fig. 25 shows the RTDS capture of DSPS 2 for the same event shown in Fig. 24. Fig. 25 shows that DSPS 2 detected the internal fault (TRPXFMR_T2 asserted). DSPS 2 closed the output contact and tripped Breakers 1, 2, and 3.

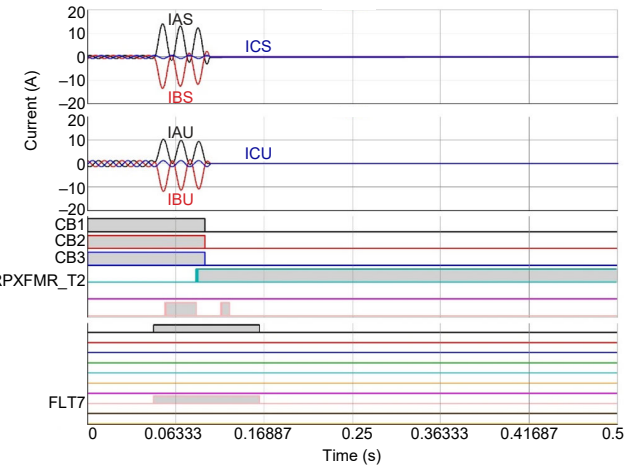

Fig. 25. Case 9: DSPS 2 Internal AG Fault at Location 7

For Case 10, we simulated an external AG fault at Location 2 that changed to an internal AG fault at Location 3.

Fig. 26 shows the RTDS capture of DSPS 1 for Case 10. An external AG fault at Location 2 was initiated at 0.05 seconds, which changed into an internal AG fault at Location 3. FLT2 asserted first, followed by FLT3. Fig. 26 shows that CON_T1 asserted during the external fault, indicating that it was an external fault. DSPS 1 remained stable. When the fault changed from external to internal, DSPS 1 detected the internal fault (CON_T1 deasserted, and TRPXFMR_T1 asserted). DSPS 1 closed the output contact and tripped Breakers 1, 2, and 3.

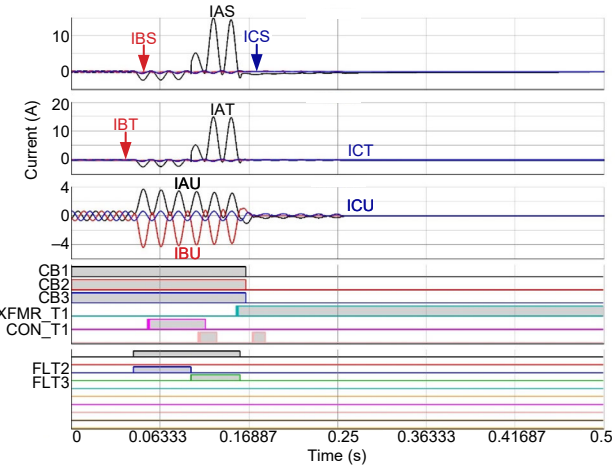

Fig. 26. Case 10: DSPS 1 External AG Fault at Location 2 Changed Into Internal AG Fault at Location 3

Fig. 27 shows the RTDS capture of DSPS 2 for the same event shown in Fig. 26. Fig. 27 shows that DSPS 2 detected that the fault changed from external to internal (CON_T2 deasserted, and TRPXFMR_T2 asserted). DSPS 2 closed the output contact and tripped Breakers 1, 2, and 3.

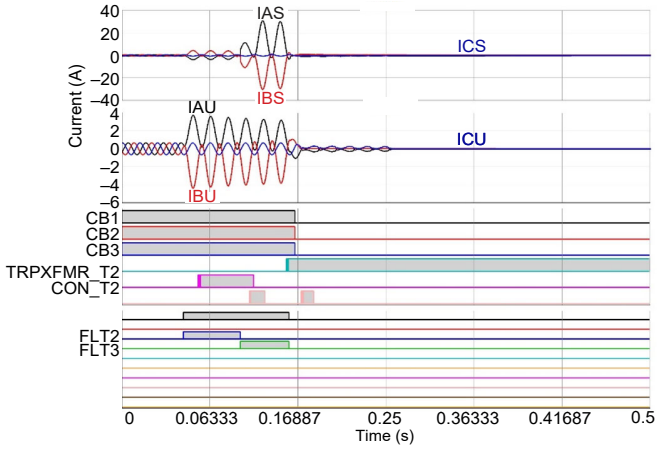

Fig. 27. Case 10: DSPS 2 External AG Fault at Location 2 Changed Into Internal AG Fault at Location 3

For Case 11, we simulated an external AG fault at Location 2 that changed to an internal AG fault at Location 3 with CT saturation.

Fig. 28 shows the RTDS capture of DSPS 1 for Case 11. An external AG fault at Location 2 was initiated at 0.05 seconds, which then changed into an internal AG fault at Location 3. Fig. 28 shows that the CTs saturated during this event (Harmonic_T1 asserted). The captures show that CON_T1 asserted during the external fault, indicating that it was an external fault. DSPS 1 remained stable. When the fault changed from external to internal, DSPS 1 detected that the fault was internal (CON_T1 deasserted, and TRPXFMR_T1 asserted). DSPS 1 closed the output contact and tripped Breakers 1, 2, and 3.

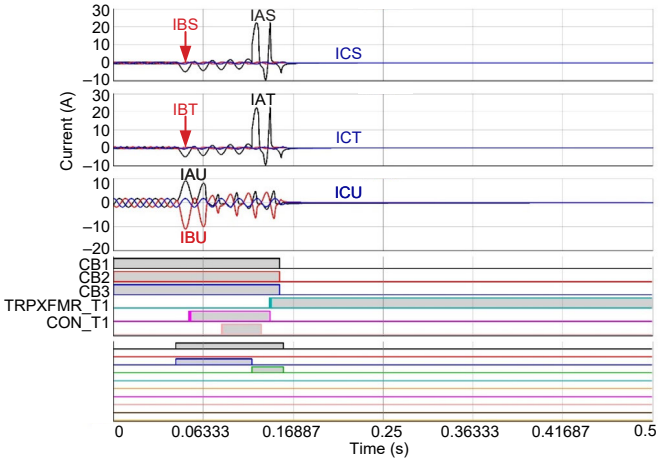

Fig. 28. Case 11: DSPS 1 External AG Fault at Location 2 Changed Into Internal AG Fault With CT Saturation at Location 3

Fig. 29 shows the RTDS capture of DSPS 2 for the same event shown in Fig. 28. Fig. 29 DSPS 2 detected that the fault changed from external to internal (CON_T2 deasserted, and TRPXFMR_T2 asserted). DSPS 2 closed the output contact and tripped Breakers 1, 2, and 3.

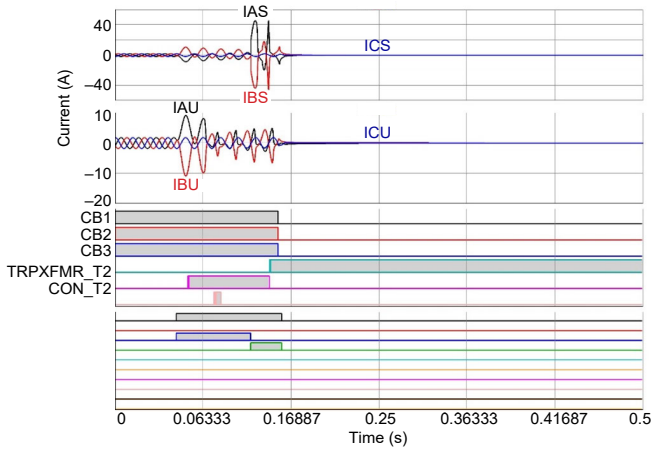

Fig. 29. Case 11: DSPS 2 External AG Fault at Location 2 Changed Into Internal AG Fault With CT Saturation at Location 3

For Case 12, we simulated an external AG fault at Location 8 that changed to an internal AG fault at Location 7.

Fig. 30 shows the RTDS capture of DSPS 1 for Case 12. An external AG fault at Location 8 was initiated at 0.05 seconds, which changed into an internal AG fault at Location 7. FLT8 asserted first, followed by FLT7. Fig. 30 shows that CON_T1 asserted during the external fault, indicating that it was an external fault. DSPS 1 remained stable. When the fault changed from external to internal, DSPS 1 detected that the fault was internal (CON_T1 deasserted, and TRPXFMR_T1 asserted). DSPS 1 closed the output contact and tripped Breakers 1, 2, and 3.

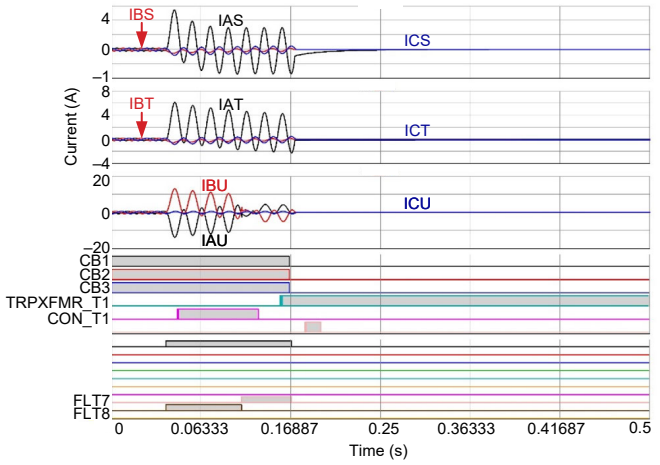

Fig. 30. Case 12: DSPS 1 External AG Fault at Location 8 Changed Into Internal AG Fault at Location 7

Fig. 31 shows the RTDS capture of DSPS 2 for the same event shown in Fig. 30. Fig. 31 shows that DSPS 2 detected that the fault changed from external to internal (CON_T2 deasserted, and TRPXFMR_T2 asserted). DSPS 2 closed the output contact and tripped Breakers 1, 2, and 3.

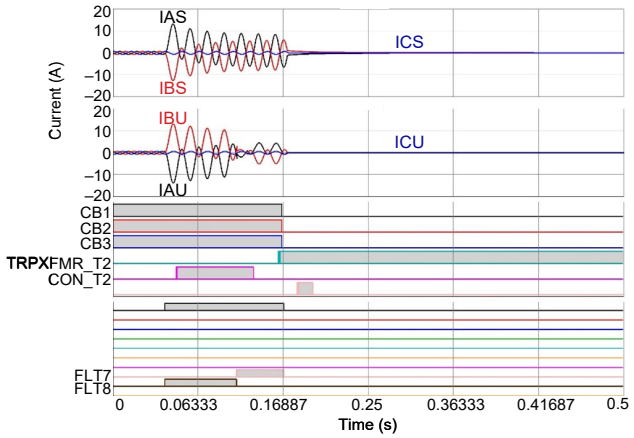

Fig. 31. Case 12: DSPS 2 External AG Fault at Location 8 Changed Into Internal AG Fault at Location 7

For Case 13, we simulated an external AG fault at Location 8 that changed to an internal AG fault at Location 7 with CT saturation.

Fig. 32 shows the RTDS capture of DSPS 1 for Case 13. An external AG fault at Location 8 was initiated at 0.05 seconds, which then changed into an internal AG fault at Location 7. Fig. 32 shows that the CTs saturated during this event (Harmonic_T1 asserted). CON_T1 asserted during the external fault, indicating that it was an external fault. DSPS 1 remained stable. When the fault changed from external to internal, DSPS 1 detected that the fault was internal (CON_T1 deasserted, and TRPXFMR_T1 asserted). DSPS 1 closed the output contact and tripped Breakers 1, 2, and 3.

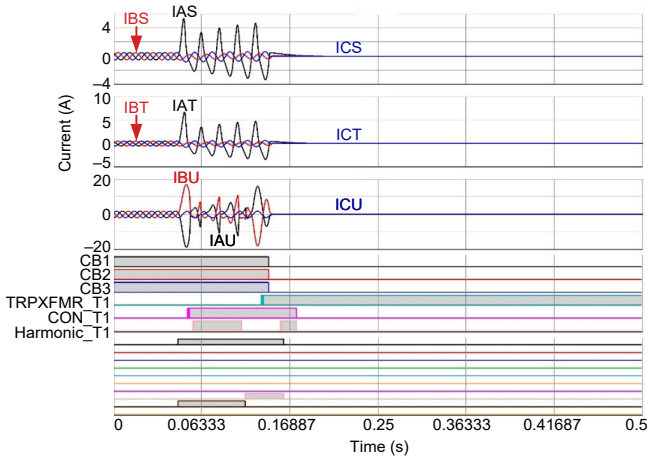

Fig. 32. Case 13: DSPS 1 External AG Fault at Location 8 Changed Into Internal AG Fault With CT Saturation at Location 7

Fig. 33 shows the RTDS capture of DSPS 2 for the same event shown in Fig. 32. Fig. 33 shows that DSPS 2 detected that the fault changed from external to internal (CON_T2 deasserted, and TRPXFMR_T2 asserted). DSPS 2 closed the output contact and tripped Breakers 1, 2, and 3.

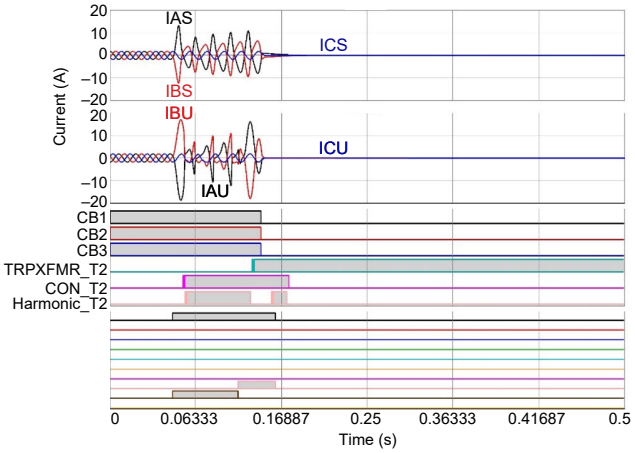

Fig. 33. Case 13: DSPS 2 External AG Fault at Location 8 Changed Into Internal AG Fault With CT Saturation at Location 7

For Case 14, all breakers were open. Then, we closed Breaker 1 at the zero-degree point-on-wave bus voltage. Within a couple of cycles, we added an internal AG fault at Location 3.

Fig. 34 shows the RTDS capture of DSPS 1 for Case 14. In this case, Breaker 1 was closed (CB1 asserted) at 0.05 seconds, and an internal AG fault at Location 3 was initiated at 0.07 seconds. When the fault changed during inrush, DSPS 1 detected an internal fault (TRPXFMR_T1 asserted). DSPS 1 closed the output contact and tripped Breaker 1.

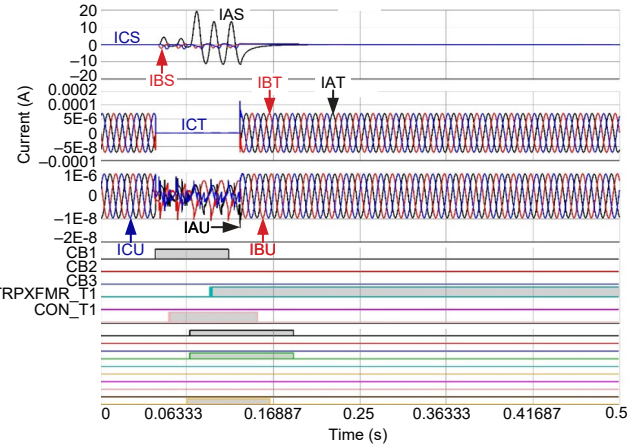

Fig. 34. Case 14: DSPS 1 Inrush Current Followed by Internal AG Fault at Location 3

Fig. 35 shows the RTDS capture of DSPS 2 for the same event shown in Fig. 34. When the fault changed during inrush, DSPS 2 detected an internal fault (TRPXFMR_T2 asserted). DSPS 2 closed the output contact and tripped Breaker 1.

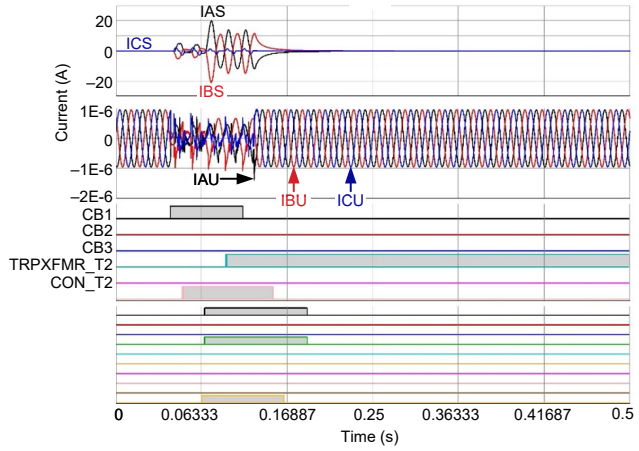

Fig. 35. Case 14: DSPS 2 Inrush Current Followed by Internal AG Fault at Location 3

For Case 15, all breakers were open. Then, we closed Breaker 1 at the zero-degree point-on-wave bus voltage. Within a couple of cycles, we added an internal AG fault at Location 7.

Fig. 36 shows the RTDS capture of DSPS 1 for Case 15. Breaker 1 was closed (CB1 asserted) at 0.05 seconds, and an internal AG fault at Location 7 was initiated at 0.07 seconds. When the fault changed during inrush, DSPS 1 detected an internal fault (TRPXFMR_T1 asserted). DSPS 1 closed the output contact and tripped Breaker 1.

Fig. 37 shows the RTDS capture of DSPS 2 for the same event shown in Fig. 36. Fig. 37 shows that DSPS 2 detected that the fault changed during inrush (TRPXFMR_T2 asserted). DSPS 2 closed the output contact and tripped Breaker 1.

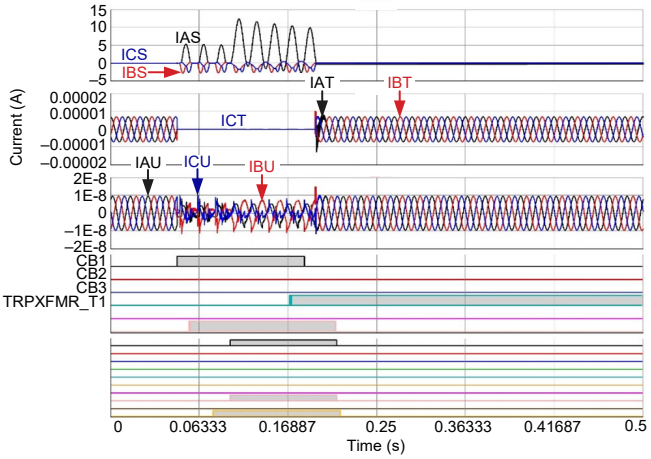

Fig. 36. Case 15: DSPS 1 Inrush Followed by Internal AG Fault at Location 7

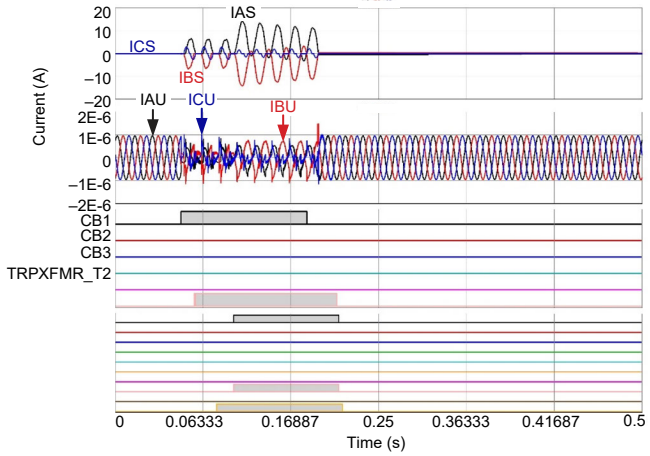

Fig. 37. Case 15: DSPS 2 Inrush Followed by Internal AG Fault at Location 7

VI. Protection Design

In an ideal case, the resiliency transformer would replace a failed power transformer without modifying the existing protection system. However, most of the power transformers in Con Edison systems were installed decades ago and are protected by electromechanical differential relays.

A modern microprocessor-based transformer differential relay is essential to provide a balance of sensitivity and security to this application. As mentioned in Section III, a modern microprocessor-based transformer differential relay with its new remote data acquisition feature was selected to protect the resiliency transformer. Two sets of MUs were installed inside the transformer cabinet. Each MU is configured with multiple CT/potential transformer (PT) cards, a digital input card, and a digital output card. The MUs obtain data from the resiliency transformer bushing CTs and send it over the EtherCAT fiber-optic cables to the remote transformer relays.

To have flexibility and high mobility like the resiliency transformer, the relay was installed in an outdoor mobile relay panel, with ac/dc test switches, a lockout relay, and so on. Each protection component installed inside the mobile relay panel provided an independent transformer protection system to account for any substation events that could cause the existing transformer protection system component to fail. Fig. 38 shows two sets of mobile relay panels.

Fig. 38. Mobile Relay Panels

To account for cases where the transformer differential protective zone was not established from the transformer bushing CTs, another set of MUs was installed inside the mobile relay panel. The mobile relay panel can be located inside or adjacent to the existing relay house, and it can obtain the CT inputs and pick up the dc trip circuit from there. Fig. 39, Fig. 40, and Fig. 41 provide some relay and MU connection examples.

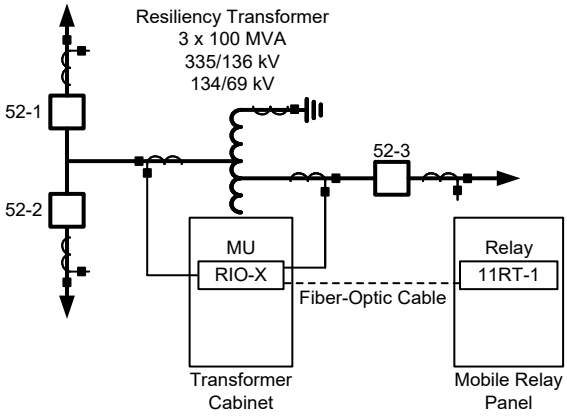

Fig. 39. Connection 1 – RIO-X and 11RT-1

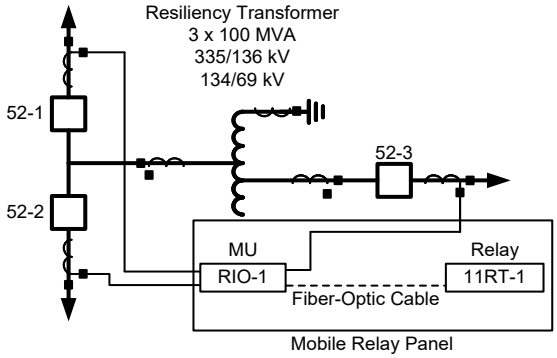

Fig. 40. Connection 2 – RIO-1 and 11RT-1

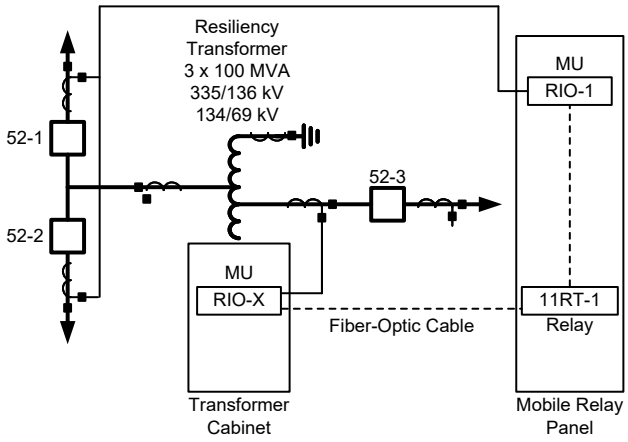

Fig. 41. Connection 3 – RIO-X, RIO-1, and 11RT-1

As discussed in Section III, both the relay and its MU are equipped with digital I/O. Because the relay and its MU can be located in various places inside a station, the digital secondary system can collect resiliency transformer trouble alarms and metering data and bring them to a station RTU via the relay. Note that the resiliency transformer has its own primary data concentrator within its control cabinet, and the digital secondary system can be used as a backup data concentrator.

VII. Project Design and Demonstration Preparation

The resiliency transformer demonstration took place at a 345 kV outdoor substation in Staten Island, New York. Proper planning, transportation, and manpower were essential to successfully install the resiliency transformer in time for the demonstration. The purpose of the demonstration was to replace an existing 328 MVA, 345/138 kV autotransformer with a resiliency transformer at full load to determine its feasibility in the system.

The engineering design phase was also essential to expedite the demonstration. Each resiliency transformer component had to be arranged and laid out properly to meet the electrical clearances. All of the components needed to be within range of the demonstration site for a quick and efficient installation. The resiliency transformer components include three single-phase transformers (approximately 30 feet in length, 23 feet in height, and 11 feet wide), control cabinets for each unit, a main control cabinet, mobile pothead structures, and mobile relay panels.

For this demonstration, the high-side connections to the existing steel bus were made with 1590 MCM ASCR cable per phase to the primary resiliency transformer air bushings. Each single-phase transformer was placed meticulously in order to maintain a 15-foot phase-to-phase electrical clearance and a 9-foot phase-to-ground clearance to the existing bus. Scaled layout drawings were created to determine the best possible arrangement to maintain the electrical clearances (Fig. 42).

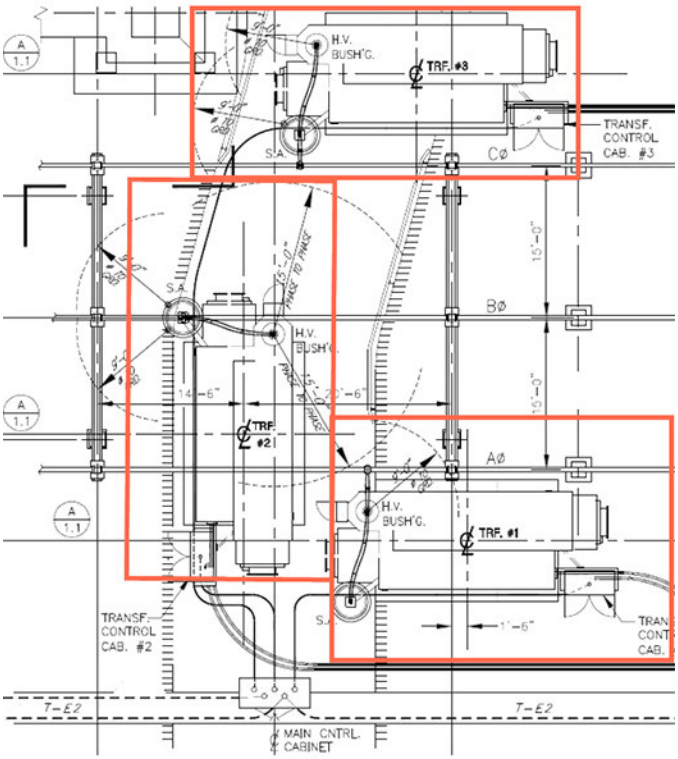

Fig. 42. Scaled Drawing for Resiliency Transformer Demonstration

The mobile pothead structures were set on 1.5-inch steel plates placed under each phase of the 138 kV low-side overhead bus. Terminations to the bus were made with 1590 MCM ACSR flexible cable. These pothead structures were designed with two pairs of terminators made from silicone rubber. Each pothead structure phase required a pair of 750 MCM solid dielectric feeder cables to terminate into the pothead structures. From these structures, proprietary cable connectors were used to plug into each single-phase resiliency transformer. The mobile pothead structure placement was essential not only for the electrical clearances, but also to provide adequate spacing for the dielectric feeder cables that connect to each single-phase resiliency transformer. The neutral and tertiary connections were required because the transformers were single phase. These connections were made using plug connectors. The technology of the plug connectors ensured quick installation as opposed to tediously terminating each wire to terminal blocks (see Fig. 43).

The main transformer control cabinet is essential for the safety, integrity, and monitoring of the energized resiliency transformers. Each transformer is equipped with a control cubicle connecting to the main control cabinet, so correct cabinet placement was crucial. The control cubicles are attached to the tank by using antivibration mountings. One main control cubicle was installed once for all three transformers. The main control cubicle was arranged separate from the transformers. The control cubicles were connected together with cables. Therefore, respective sockets were provided on the cubicles where the cables could be plugged in.

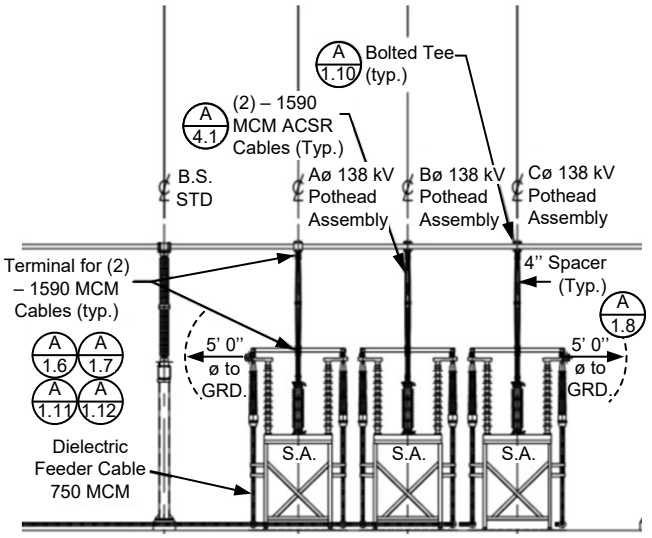

Fig. 43. Three Single-Phase Pothead Assembly Structures

Five different cable types (all with varying lengths) were necessary to connect the cubicles. Each cable is marked with the cable type and the cable number. The main control cabinet was placed within the cable limited cable range. Main connections from the substation to the main control cabinet included power, alarms, and controls, which were all easily installed because of the cable raceway system (see Fig. 42).

Two first and second line mobile relay panels were designed to provide additional protection for the resiliency transformer. These were built specifically for outdoor use and were made from outdoor-rated stainless steel, mimicking the typical relay cabinets in Con Edison's substations. These mobile relay panels were essential to provide differential protection, as described in Section VI. The mobile relay panels were designed with a bottom entry opening for easy cable management in and out of the panel. These mobile relay panels helped make the installation quicker and more reliable, without having to rely on existing relays in the substation.

With all the major components prepared, the installation phase was quick. Based on this demonstration, approximately three days of manpower was required to install all of the components. Typical transformer replacement takes three to four weeks, and procuring a 328 MVA autotransformer takes over a year. With the proper planning and cable connection technology, mobile relay panels, and pothead structures, the typical installation time was drastically reduced.

VIII. Protection System Bench Test

The Technical Applications (Tech Apps) group is a subgroup within Con Edison's Protecting Systems Testing Department. Tech Apps has always brought significant value to Con Edison because they have helped reduce outage times and recurring problems associated with equipment commissioning. The group's primary responsibilities are to review relay settings and associated drawings and tripping schemes, understand the intent of the relay scheme and create computer-aided tests to bench test the relays. The Tech Apps group creates and

performs test plans associated with microprocessor-based relays.

Bench testing involves simulating specific fault conditions by injecting voltages and currents into relays and observing their responses. Fig. 44 shows one of the bench testing setups used to test the relay systems that protect the resiliency transformer. The bench test setup included a test set, an MU, and a microprocessor-based transformer differential relay with remote data acquisition features.

The test set provided the voltage and current sources. The test involved injecting current into the MU and monitoring the relay output contacts for operation. The relay was connected to the MU via an EtherCAT fiber-optic cable. This connection uses less copper and provides faster restoration if equipment needs to be replaced. The goal was to position the MU near the CTs that are part of the transformer protection scheme, minimizing the amount of copper required. In addition, another MU was included in the mobile relay panel to provide an alternative configuration.

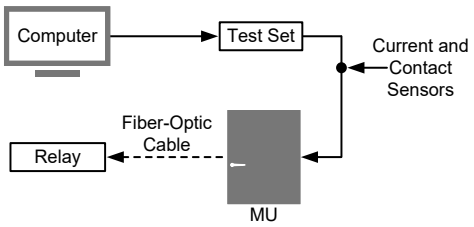

Fig. 44. Relay Bench Testing Setup 1

Differential elements are the primary protection for the resiliency transformer. To prepare for the transformer demonstration, restrained differential element 87R, unrestrained differential element 87U, and negative-sequence differential element 87Q were enabled and tested in the transformer relay.

For the restrained 87R element, we tested a pickup current of 1.130 A secondary. A pickup test was performed on all three phases and at all three windings of the relay. In addition to the pickup test, slope tests were performed that were simulated on and below the sensitive slope (Slope 1) and the secure slope (Slope 2). These tests confirmed that the relay responded correctly. Harmonic restraint is enabled in the relay to provide security to the restrained 87R element during inrush conditions.

For the unrestrained 87U element, we tested a pickup current of 17.87 A secondary. Similar to the previous test, this was performed on all three phases and at all three windings of the relay. Essentially, this element will operate once the current exceeds the pickup value. No slope testing was involved.

For the negative-sequence 87Q element, we tested a pickup current of 0.390 A secondary ($3I_2$). The point of this test was to monitor any negative-sequence current within the windings. If the negative-sequence 87Q element operated, an alarm would operate, indicating that there was possible arcing (turn-to-turn fault) within the transformer winding. In addition to the pickup test, slope tests were performed, which were simulated on and below Slopes 1 and 2. These tests confirmed that the relay responded correctly.

Con Edison Engineering and Tech Apps groups have experience with the conventional model of the microprocessor-based relay. From the Engineering group standpoint, setting this relay with its remote data acquisition feature compared with its conventional model makes no difference. Since the engineers are familiar with this relay, they could create settings files using this protection system when deploying the resiliency transformer.

Testing was modified depending on the transformer cabinet and the mobile relay panel (see Fig. 39, Fig. 40, and Fig. 41) configuration and placement. In the scenario where the relay protection resides in one place (see Fig. 44), the commissioning test can be performed locally in the relay panel. When the relay and MU are located in different locations (see Fig. 45), a satellite test is required. With the help of GPS satellite time, current injection can be synchronized for all the test sets as if both the relay and MU are next to each other (see Fig. 45).

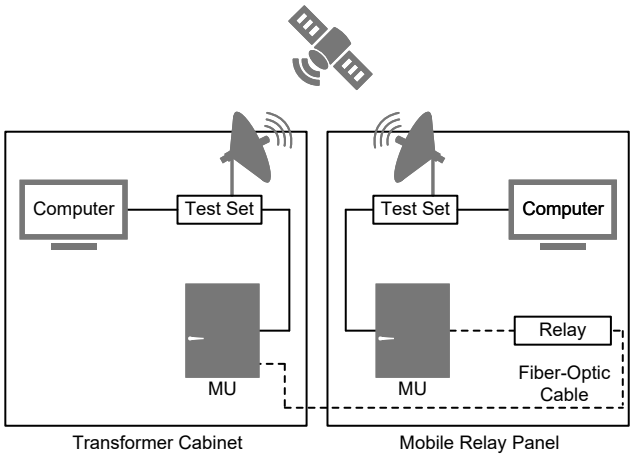

Fig. 45. Relay Bench Testing Setup 2

To validate the performance of this relay with its new remote data acquisition feature, bench tests were performed on both the conventional model and the remote data acquisition model with the same settings and test plans. Both pickup and timing tests were performed, and Table I and Table II show the test results.

TABLE I
VARIOUS PICKUP TESTS FOR PERCENT ERROR COMPARISON

Differential Element Test	Conventional Model (%)	Remote Data Acquisition Model (%)
Restrained 87R (with one restraint current)	0	0
Restrained 87R on Slope 1 (with two restraint currents)	3.27	3.74
87U	–1.16	0.78
Negative-sequence 87Q (with one restraint current)	2.56	2.56
Negative-sequence 87Q on slope (with two restraint currents)	–3.40	–3.40

TABLE II
VARIOUS OPERATING TIME TESTS COMPARISON (AVERAGE OF EIGHT TESTS)

Differential Element Test	Conventional Model (cycles)	Remote Data Acquisition Model (cycles)
Restrained	1.43	1.47
Unrestrained	0.93	0.97

Table I shows that the remote data acquisition model does not seem to introduce any additional percent error compared with the conventional model.

The timing tests for both differential elements were repeated eight times. Table II shows that the averages of the two element operating times of the remote data acquisition model were slightly (0.04 cycles) more than the conventional model.

IX. FIELD COMMISSIONING

On January 13, 2017, the resiliency transformer was installed and energized in a selected Con Edison transmission substation as a public demonstration. This demonstration involved replacing an existing 328 MVA, 345/138 kV autotransformer with the resiliency transformer that would re-pick up the load for seven days.

Events were triggered in the new transformer relays to observe the relay performance and load conditions while the resiliency transformer was in service. Fig. 46 shows one of the triggered event files, where three-phase currents were balanced and no standing differential currents (IOP) were identified.

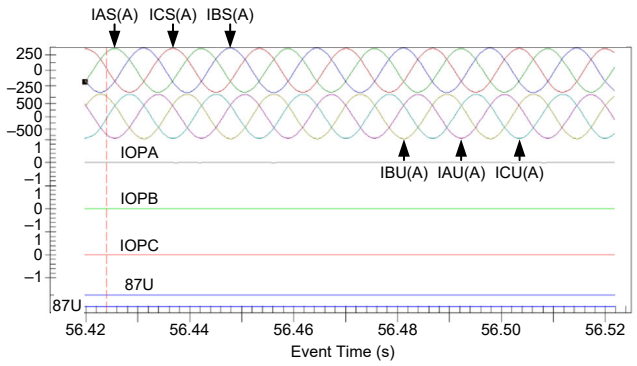

Fig. 46. Triggered Event Report

After energization, the transmission operator adjusted the adjacent phase angle regulator and forced 240 MW to flow through the resiliency transformer. The transformer remained in service for seven days. Then, it was disconnected, shipped to the designated location, and armed for a future transformer failure replacement.

X. CONCLUSION

Losing any large transmission substation results in severe issues with system power flows and stability that serve critical demand in Con Edison's service territory, potentially impacting many customers. As a result, alternative means to restore power to these customers is a major priority to prevent a catastrophic event. Every utility is required to have a contingency plan to restore the power system expeditiously and keep their customer average interruption duration index (CAIDI) metrics and customer minutes of interruption (CMI) low.

Losing a large transmission-level power transformer places the system into a critical contingency condition. The power system stability limit will be derated, and electric service could be interrupted if another critical contingency occurs after the first transformer failure. The large power transformer must be restored quickly to ensure that the power system returns to normal operating conditions. This is best achieved by using resiliency transformers for rapid restoration. Pairing modern digital secondary systems with a resiliency transformer can make the NYC power grid more robust and reliable.

XI. REFERENCES

[1] Consolidated Edison Company of New York, Inc., "How We Source Our Energy." Available: https://www.coned.com/en/our-energy-future/how-we-source-our-energy/electricity.

[2] The New York Independent System Operator (NYISO), Inc., "2018 Power Trends: New York's Dynamic Power Grid," May 2018. Available: https://home.nyiso.com/wp-content/uploads/2018/05/2018-Power-Trends_050318.pdf.

XII. BIOGRAPHIES

Ed W. Chen graduated from City University of New York with a Bachelor of Science in Electrical Engineering Science and from Worcester Polytechnic Institute with a Master of Science in Electrical and Computer Engineering. Ed joined National Grid New York in 2010. In 2012, he became a Relay Protection Engineer in their Protection Analysis and Relay Project Engineering groups. In 2016, Ed joined Consolidated Edison Company of New York, Inc. and continues to work there as a Relay Protection Engineer. Ed is a registered Professional Engineer in the state of New York.

Anastasia O'Malley holds an MSEE from Manhattan College, a BSME from Rutgers University, and an MBA from Fordham University. She is a Project Manager in the substation equipment section of Central Engineering and provides technical guidance on the purchase, installation, maintenance, and replacement of the power transformer fleet at Consolidated Edison Company of New York, Inc. She is an IEEE/PES Transformer Committee member and has served as an officer of the Doble Engineering Company Transformer Committee.

Nadia Ali graduated from New York Institute of Technology with a Bachelor of Science in Electrical and Computer Engineering. Nadia worked in engineering consulting firms as an Electrical Design Engineer and Project Engineer for several high-rise commercial buildings. In 2014, Nadia joined Consolidated Edison Company of New York, Inc. as an Engineer and currently is an Engineering Design Supervisor in the Equipment & Field Engineering section of Central Engineering. Her work involves engineering and design for substation equipment replacement and major reliability projects for the transmission system. Nadia is an IEEE member.

Leslie Philp holds a BEEE from the City College of the City University of New York, an MSEE from the Polytechnic Institute of New York University, and an MBA from Fordham University. He currently works in the Protective Systems Testing Department at Consolidated Edison Company of New York, Inc., where he is responsible for testing and commissioning advanced microprocessor relays. Leslie has worked in relay protection, power systems design and analysis, project management, and cable systems testing. He is one of three inventors who filed a patent application for a "System and Method of Monitoring a Utility Structure" since 2017.

Diego Pichardo received his B.S. degree in Electrical Engineering from the University of Rhode Island in 2005. He joined Consolidated Edison Company of New York, Inc. in 2006 as an Electrical Technician. In 2009, he became a Senior Electrical Technician in the Protective Systems and Testing (PST) Department. In 2013, he joined the Technical Application group as a Technical Supervisor within PST, and he is currently the Manager of the Technical Applications Group within PST.

Fabricio Mantilla graduated from Binghamton University with a Bachelor of Science in Electrical Engineering and from Fordham University with an MBA. He worked for consulting firms, serving clients from the U.S. Navy, PSE&G, and Constellation Energy Company. He joined Consolidated Edison Company of New York, Inc. in 2012 as an Electrical Engineer, supervising projects for four years. After that, he moved to another division of Con Edison as a Technical Applications Engineer and was responsible for the testing and approving of multiple relays installed in Con Edison's system.

Rogerio C. Scharlach received his BSEE in 1991 from the Mackenzie Presbyterian University in São Paulo, Brazil. After graduation, he worked nearly 13 years at Siemens in Brazil and then in the United States. At Siemens, he was a Commissioning and Field Service Engineer in the areas of power generation, transmission, and distribution. He joined Schweitzer Engineering Laboratories, Inc. in 2005, where he currently works as a Principal Engineer in Alpharetta, Georgia. He is an IEEE member.

Satish Samineni received his Bachelor of Engineering degree in Electrical and Electronics Engineering from Andhra University, Visakhapatnam, India, in 2000. He received his Master's degree in Electrical Engineering from the University of Idaho in 2003. Since 2003, he has worked at Schweitzer Engineering Laboratories, Inc. in Pullman, WA, where he is a Senior Research Engineer in the Research and Development Division. He has authored or coauthored several technical papers and holds multiple U.S. patents. His research interests include power electronics and drives, power system protection, synchrophasor-based control applications, and power system stability. He is a registered professional engineer in the state of Washington and a senior member of IEEE.